First-principles Calculations of the Diffusivity of Interstitial Helium-3 in Alpha-U

Jae-Hyuk Kim [a], Jae-Uk Lee [b], Min Ho Chang [b], Takuji Oda [a*]
[a] *Department of Nuclear Engineering, Seoul National University, 1, Gwankak-ro, Gwanak-gu, Seoul (08826), Republic of Korea*
[b] *Korea Institute of Fusion Energy, 169-148, Gwahak-ro, Yuseong-gu, Daejeon (34133), Republic of Korea*
**Corresponding Author: oda@snu.ac.kr*

1. Introduction

Uranium (alpha-U) is currently planned to be used as the tritium storage material in the form of uranium tritide (UT_3) for the tritium storage and delivery system (SDS) of the International Thermonuclear Experimental Reactor (ITER) fuel cycle due to its successful capacities to retain tritium at room temperature with a low decomposition pressure and provide stable delivery in the 700-800 K range [1], [2]. During the tritium storage period, helium-3 is produced in UT_3 by beta decay of tritium with a half-life of 12.3 years. A formidable issue of produced helium is that it hardly leaves the host material by heating even above the decomposition temperature of UT_3 and the major release of helium requires heating above 800-1000 K [3]. After the desorption of tritium from the host material, due to its low solubility, helium is anticipated to form bubbles in alpha-U [4]. Although the accumulated helium in alpha-U would affect the storage and delivery performance of the tritium SDS, the behavior of helium in alpha-U is yet to be sufficiently studied.

In this work, the interstitial helium diffusion in alpha-U is studied by computational and theoretical methods as one of the fundamental properties that determine the behavior of helium accumulated in alpha-U. Specifically, the diffusion mechanism of helium in alpha-U is identified and the diffusion coefficient is determined based on density functional theory (DFT) calculations. This fundamental data on the mobility of helium is expected to contribute to the development of uranium metal fuels for advanced nuclear reactors as well [5] in terms of understanding the behavior of noble gases.

2. Methods and Computational Details

2.1 DFT calculation settings

First-principles calculations were performed based on DFT by the Vienna Ab initio Simulation Package (VASP) [6]. The valence and semi-core electrons for U ($6s^26p^65f^36d^17s^2$) and He ($1s^2$) were described by plane waves with an energy cutoff of 480 eV under the energy convergence criterion of 1×10^{-8} eV for most calculations. The effect of the core electrons was treated with the projector augmented wave (PAW) method [7], and the Perdew-Burke-Ernzerhof (PBE) functional of the generalized gradient approximation (GGA) [8] was used to evaluate the exchange-correlation energy. The Hubbard U correction was applied to the uranium *f*-orbital in the formalism proposed by Dudarev *et al.*[9], [10], with the U parameter of 0.6 eV, which was optimized for uranium hydride [11]. Methfessel and Paxton's first-order smearing method [12] was used with a 0.2 eV smearing width to address the partial occupancies of energy levels. All calculations were performed in non-spin-polarized conditions as the magnetic moments of the systems were virtually zero and there were no energy differences between the non-spin-polarized and spin-polarized calculations.

2.2 Crystallographic Structure of Alpha-U and the Stability of Interstitial Helium

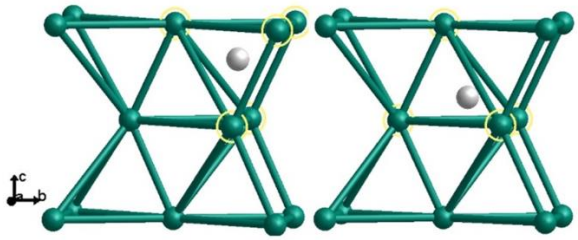

Figure 1. Square-pyramidal interstitial site (left) and tetrahedral interstitial site (right) in alpha-U. White spheres represent helium atoms at these interstitial sites, and green spheres correspond to uranium atoms.

The stable phase of uranium is the alpha phase (space group 63; Figure 1) [13] under the planned operation conditions of the ITER-SDS. Before evaluating the migration properties of helium, we tested the validity of the numerical parameters for the DFT calculations of the lattice constants, the vacancy formation energy, and the interstitial helium formation energy in alpha-U. The lattice constants were calculated in a conventional unit cell (consisting of 4 U atoms) with an energy cutoff of 600 eV and a 28×14×16 gamma-centered k-point sampling mesh, and the other properties were determined in 5×3×3 supercells (consisting of 180 U atoms). The numerical errors induced by the cutoff energy and k-point sampling grid were verified to be less than 0.001 Å for the lattice constant and on the order of 0.02 eV and 0.01 eV for the vacancy formation and the interstitial helium formation energy, respectively.

The lattice constants of alpha-U calculated with the above settings show good agreement with experimental

results, as shown in Table 1. Compared with the previous DFT calculation results using GGA functionals (PBE and PW91), the agreement with experiments on the lattice constants is slightly improved by the Hubbard U correction, which partly justifies the use of the Hubbard U correction in this study.

Table 1. Comparison of the lattice constants and the vacancy formation energy with previous studies. The experimental lattice constants were obtained at room temperature [14] and 4.2 K [15].

	Method	*a* (Å)	*b* (Å)	*c* (Å)	E_f^{vac} (eV)
This work	GGA+U (PBE)	2.8320	5.8562	4.9346	1.69[a]
Sturcken [14]	experimental	2.854	5.869	4.955	-
Lloyd [15]	experimental	2.8444	5.8689	4.9316	-
Huang [16]	GGA (PW91)	2.798	5.866	4.899	1.69[a], 1.75[b]
Söderlind [17]	FP-LMTO	2.845	5.818	4.996	-
Taylor [18]	GGA (PW91)	2.797	5.867	4.893	1.95[c]
Beeler [19]–[21]	GGA (PBE)	2.793	5.849	4.894	1.86[c], 1.69[a]

[a] 5×3×3 supercell; [b] 6×3×3 supercell; [c]4×2×3 supercell.

The vacancy formation energy was calculated by

$$E_f^{vac} = -\left[\frac{N-1}{N}E(U_N)\right] + E(U_{N-1}), \quad (1)$$

where $E(U_N)$ and $E(U_{N-1})$ are the potential energies of perfect alpha-U lattice in a supercell containing N uranium atoms and of that of the same size with a vacancy, respectively. Our result, 1.69 eV with N=180, is comparable to the results from previous calculations [16], [18]–[20].

We identified there are two stable interstitial sites for helium in alpha-U: the square pyramidal site (sqpy-site) and the tetrahedral site (tet-site), as shown in Figure 1 [22].

The formation energy of interstitial helium was calculated by

$$E_f^{int,He} = -[E(U_N) + E(He)] + E(U_N He_1), \quad (2)$$

where $E(U_N)$ and $E(U_N He_1)$ are the potential energies of alpha-U lattice in a supercell consisting of N uranium atoms without and with interstitial helium, respectively, and $E(He)$ is the potential energy of a helium atom in a vacuum. The formation energy of interstitial helium was determined to be 3.666 eV at an sqpy-site, which agrees well with the result of the calculation by Beeler *et al.* [23] (3.63 eV), and that at a tet-site calculated to be 3.670 eV.

2.3 Migration Paths of Interstitial Helium in Alpha-U

With the two interstitial sites described in the previous section, we constructed three types of migration, namely, SS migration, TT migration, and ST migration, which correspond to migration from an sqpy-site to an sqpy-site, from a tet-site to a tet-site, and from an sqpy-site to a tet-site, respectively. In this work, *XYn* migration denotes the migration path that originates at the *X*-site and ends at the *n*-th neighboring *Y*-site.

The NEB method was applied to 5 images to determine the migration path and the potential energy at the transition state for each path. Migration paths up to the 7th, 4th, and 3rd neighboring sites were considered in the calculation for SS, TT, and ST migration, respectively, as these paths appeared to have reasonably short jump distances. Temperature-dependent lattice constants suggested by Lloyd *et al.*[15] were applied while constructing the NEB calculation to take into account the thermal expansion effect on the migration barrier. The results of the NEB calculations showed that some of the tested paths have multiple transition states and can be represented by a combination of other paths, each of which contains a single transition state. Hereafter, we specifically refer to a migration path that included only one transition state as a fundamental migration path.

2.4 Diffusion Coefficient Calculation

The diffusion coefficient of interstitial helium was obtained by kinetic Monte Carlo (KMC) calculations using all the fundamental migration paths. As inputs for the diffusion coefficient calculation, the migration barriers and attempt frequencies for available migration paths are needed. The migration barriers were determined by the NEB calculations, and the attempt frequencies were obtained through vibrational analysis. The vibrational analysis was performed with the harmonic approximation at the gamma point by adopting the phonopy code [24]. The Hessian was constructed by the finite displacement method with 0.015 Å displacement for 3×2×2 supercells of alpha-U

containing a single interstitial helium atom at the sqpy-site, the tet-site, or the transition state of each migration path. In the DFT calculations of the finite displacement method, 5×3×4 gamma-centered k-point grids were applied to sample the band energy.

Table 2. Fundamental migration paths identified in this study. Non-fundamental migration paths are decomposed into fundamental paths.

Migration path	Decomposition	Migration path	Decomposition
SS1	Fundamental	TT1	Fundamental
SS2	Fundamental	TT2	TS1 + ST2
SS3	ST2 + TS1	TT3	TS1 + SS1 + ST1
SS4	SS2 + SS1	TT4	TS2 + ST2
SS5	ST2 + TS2	ST1 (TS1)	Fundamental
SS6	SS1 + SS2 + SS1	ST2 (TS2)	Fundamental
SS7	ST2 + TS2 + SS1	ST3 (TS3)	ST1+TT1

Using the vibration analysis results, the temperature-dependent effective attempt frequency was obtained with Eyring's theory of activated complexes [25], which is expressed as

$$\Gamma = \frac{kT}{h}\frac{\prod_{i=1}^{3N-3} 2\sinh\left(\frac{h\nu_i^{GS}}{2kT}\right)}{\prod_{i=1}^{3N-4} 2\sinh\left(\frac{h\nu_i^{TS}}{2kT}\right)} \times e^{-\Delta E_{mig}/kT} = \nu_0(T) \times e^{-\Delta E_{mig}/kT}, \quad (3)$$

where Γ is the atomic jump rate, k is the Boltzmann constant, T is the temperature, h is the Planck constant, and ν_i^{GS} and ν_i^{TS} are the vibration frequencies of the i-th real normal modes for the ground state and transition state, respectively, in each fundamental migration path.

In the KMC simulations, the random walks of helium are regulated by the migration barriers and attempt frequencies in the event list. The random walks were repeated to simulate the diffusion process. Finally, the diffusion coefficient was calculated from the mean square displacement (MSD) using the Einstein relation

$$D = \frac{\text{MSD}}{2dt}, \quad (4)$$

where D is the diffusion coefficient, d is the dimension of interest (i.e., d=1 for 1-D diffusion and d=3 for 3-D diffusion), and t is the elapsed time of the simulation. The 3-D diffusion coefficient is equal to the average of three 1-D diffusion coefficients (D_x, D_y, D_z).

3. Results and Discussion

3.1 Migration Paths of Interstitial Helium in Alpha-U

The fundamental migration paths identified by the NEB calculation and the vibrational analysis are shown in Table 2. SS1, SS2, TT1, ST1 (TS1), and ST2 (TS2) migration were the fundamental migration paths. We confirmed that an appropriate combination of these paths can depict any kind of migration path.

3.2 Diffusion Coefficient Calculations

The KMC calculation results of the 1-D (i.e., x-, y-, and z-directions) and 3-D diffusion coefficients of interstitial helium are shown in Figure 2. By fitting the data with the Arrhenius equation, the effective migration barrier for 3-D diffusion was determined to be 0.202 eV with a pre-factor of D_0 = 9.67×10^{-4} cm^2/s. Meanwhile, significant anisotropy was observed regarding the migration direction; diffusion in z-direction was always dominant for the selected temperature range (i.e., 200-900 K), followed by x- and y-diffusion.

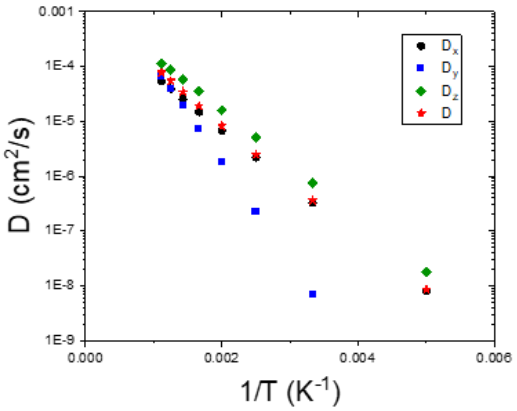

Figure 2. 1-D and 3-D diffusion coefficients of helium in alpha-U determined by KMC simulations.

Finally, since there is no experimental data available for helium diffusion in alpha-U, we compare the calculation results with experimental diffusion coefficients of other impurities in alpha-U in Figure 3. The calculated diffusion coefficient for helium is comparable with the experimental diffusion coefficient of hydrogen [26], while much smaller than the experimental diffusion coefficients of xenon [27]. The proximity of the calculated helium diffusivity and experimentally determined hydrogen diffusivity partially supports the validity of the present calculation result, considering that the diffusivity of the two elements is often comparable in metal, e.g., in bcc-W and bcc-Fe [28]–[31]. The atomic radii are 0.53 Å for hydrogen, 0.31 Å for helium, and 1.08 Å for xenon [32]–[34]. Thus, it is considered that the size of the

impurity has a large effect on the diffusivity of the impurity in alpha-U.

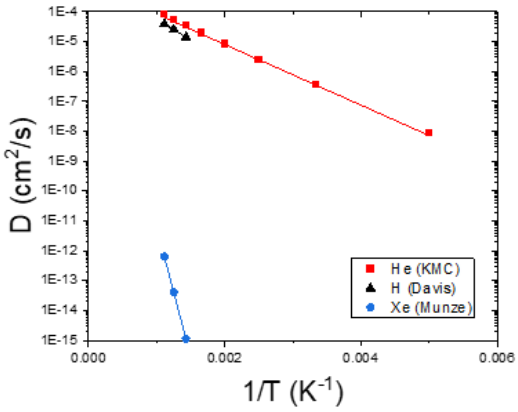

Figure 3. Comparison of the helium diffusion coefficients obtained by KMC with experimental results for hydrogen by Davis and xenon by Münze.

4. Conclusion

In this work, we studied the interstitial diffusion of helium in alpha-U using first-principles calculations and KMC simulations. The diffusion mechanism was identified and the diffusion coefficient was obtained. Significant diffusion anisotropy was observed. The relatively large value of diffusivity suggests that the release of helium from metal U would quickly occur once helium can escape from defect complexes.

REFERENCES

[1] M. Glugla *et al.*, "The ITER tritium systems," *Fusion Eng. Des.*, vol. 82, no. 5–14, pp. 472–487, 2007.

[2] T. Yamamoto, Supardjo, T. Terai, F. Ono, S. Tanaka, and M. Yamawaki, "Storage of Hydrogen Isotopes in Uranium Alloys," *Fusion Technol.*, vol. 14, no. 2P2A, pp. 764–768, 1988.

[3] B. Limacher, D. Leroy, C. Arnoux, and C. Kassel, "Helium 3 Release from Uranium Tritide," *Zeitschrift fur Phys. Chemie*, vol. 183, no. Part_1_2, pp. 465–472, 1994.

[4] W. D. Wilson, C. L. Bisson, and M. I. Baskes, "Self-trapping of helium in metals," *Phys. Rev. B*, vol. 24, no. 10, pp. 5616–5624, Nov. 1981.

[5] G. L. Hofman, S. L. Hayes, and M. C. Petri, "Temperature gradient driven constituent redistribution in U-Zr alloys," *J. Nucl. Mater.*, vol. 227, no. 3, pp. 277–286, Jan. 1996.

[6] G. Kresse and J. Furthmüller, "Efficient iterative schemes for ab initio total-energy calculations using a plane-wave basis set," *Phys. Rev. B*, vol. 54, no. 16, pp. 11169–11186, Oct. 1996.

[7] B. P.E., "Projector augmented-wave method," *Phys. Rev. B*, vol. 50, no. 24, pp. 17953–17979, 1994.

[8] J. P. Perdew, K. Burke, and M. Ernzerhof, "Generalized gradient approximation made simple," *Phys. Rev. Lett.*, vol. 77, no. 18, pp. 3865–3868, 1996.

[9] S. L. Dudarev, G. A. Botton, S. Y. Savrasov, C. J. Humphreys, and A. P. Sutton, "Electron-energy-loss spectra and the structural stability of nickel oxide: An LSDA1U study," *Phys. Rev. B*, vol. 57, no. 3, 1998.

[10] D. Nguyen-Manh and S. L. Dudarev, "Trapping of He clusters by inert-gas impurities in tungsten: First-principles predictions and experimental validation," *Nucl. Instruments Methods Phys. Res. Sect. B Beam Interact. with Mater. Atoms*, vol. 352, pp. 86–91, 2015.

[11] K. Jun, J.-U. Lee, M. H. Chang, and T. Oda, " A comparative study on modeling of the ferromagnetic and paramagnetic states of uranium hydride using a DFT+ U method ," *Phys. Chem. Chem. Phys.*, vol. 21, no. 32, pp. 17628–17639, 2019.

[12] M. Methfessel and A. T. Paxton, "High-precision sampling for Brillouin-zone integration in metals," *Phys. Rev. B*, vol. 40, no. 6, pp. 3616–3621, Aug. 1989.

[13] C. W. Jacob and B. E. Warren, "The Crystalline Structure of Uranium," *J. Am. Chem. Soc.*, vol. 59, no. 12, pp. 2588–2591, 1937.

[14] E. F. Sturcken, "The atomic position parameter in alpha uranium," *Acta Crystallogr.*, vol. 13, no. 10, pp. 852–852, 1960.

[15] L. T. Lloyd and C. S. Barrett, "Thermal expansion of alpha uranium," *J. Nucl. Mater.*, vol. 18, no. 1, pp. 55–59, Jan. 1966.

[16] G. Y. Huang and B. D. Wirth, "First-principles study of bubble nucleation and growth behaviors in α U-Zr," *J. Phys. Condens. Matter*, vol. 24, no. 41, 2012.

[17] P. Söderlind, "First-principles elastic and structural properties of uranium metal," *Phys. Rev. B - Condens. Matter Mater. Phys.*, vol. 66, no. 8, pp. 851131–851137, 2002.

[18] C. D. Taylor, "Evaluation of first-principles techniques for obtaining materials parameters of α - uranium and the (001) α -uranium surface," *Phys. Rev. B - Condens. Matter Mater. Phys.*, vol. 77, no. 9, pp. 1–9, 2008.

[19] B. Beeler, B. Good, S. Rashkeev, C. Deo, M. Baskes, and M. Okuniewski, "First principles calculations for defects in U," *J. Phys. Condens. Matter*, vol. 22, no. 50, p. 505703, Dec. 2010.

[20] B. Beeler, K. Mahbuba, Y. Wang, and A. Jokisaari, "Determination of Thermal Expansion, Defect Formation Energy, and Defect-Induced Strain of α-U Via ab Initio Molecular Dynamics," *Front. Mater.*, vol. 8, no. June, pp. 1–9, Jun. 2021.

[21] B. Beeler, C. Deo, M. Baskes, and M. Okuniewski, "First principles calculations of the structure and elastic constants of α, β and γ uranium," *J. Nucl. Mater.*, vol. 433, no. 1–3, pp. 143–151, 2013.

[22] C. D. Taylor and R. Scott Lillard, "Ab-initio calculations of the hydrogen–uranium system: Surface phenomena, absorption, transport and trapping," *Acta Mater.*, vol. 57, no. 16, pp. 4707–4715, Sep. 2009.

[23] B. Beeler, B. Good, S. Rashkeev, C. Deo, M. Baskes, and M. Okuniewski, "First-principles calculations of the stability and incorporation of helium, xenon and krypton in uranium," *J. Nucl. Mater.*, vol. 425, no.

1–3, pp. 2–7, 2012.
[24] A. Togo and I. Tanaka, “First principles phonon calculations in materials science,” *Scr. Mater.*, vol. 108, pp. 1–5, 2015.
[25] H. Eyring, “The activated complex in chemical reactions,” *J. Chem. Phys.*, vol. 3, no. 2, pp. 63–71, 1935.
[26] W. D. Davis, “Solubility, Determination, Diffusion and Mechanical Effects of Hydrogen in Uranium,” Niskayuna, NY, Aug. 1956.
[27] R. Münze, O. Hladik, S. A. Marei, S. El-Bayoumy, and M. El-Garhy, “133Xe release during post-irradiation annealing of uranium metal in the presence of a constant volume of air,” *J. Radioanal. Chem.*, vol. 45, no. 1, pp. 141–146, Mar. 1978.
[28] D. Stewart, Y. Osetskiy, and R. Stoller, “Atomistic studies of formation and diffusion of helium clusters and bubbles in BCC iron,” *J. Nucl. Mater.*, vol. 417, no. 1–3, pp. 1110–1114, 2011.
[29] Y. He, Y. Li, C. Chen, and H. Yu, “Diffusion coefficient of hydrogen interstitial atom in A-Fe, Γ-Fe and ε-Fe crystals by first-principle calculations,” *Int. J. Hydrogen Energy*, vol. 42, no. 44, pp. 27438–27445, 2017.
[30] H. Wen and C. H. Woo, “Temperature dependence of enthalpies and entropies of formation and migration of mono-vacancy in BCC iron,” *J. Nucl. Mater.*, vol. 455, no. 1–3, pp. 31–36, Dec. 2014.
[31] X. Yang and W. O. Oyeniyi, “Kinetic Monte Carlo simulation of hydrogen diffusion in tungsten,” *Fusion Eng. Des.*, vol. 114, pp. 113–117, 2017.
[32] E. Clementi and D. L. Raimondi, “Atomic Screening Constants from SCF Functions,” *J. Chem. Phys.*, vol. 38, no. 11, pp. 2686–2689, Jun. 1963.
[33] E. Clementi, D. L. Raimondi, and W. P. Reinhardt, “Atomic Screening Constants from SCF Functions. II. Atoms with 37 to 86 Electrons,” *J. Chem. Phys.*, vol. 47, no. 4, pp. 1300–1307, Aug. 1967.
[34] J. C. Slater, “Atomic shielding constants,” *Phys. Rev.*, vol. 36, no. 1, pp. 57–64, 1930.